Grinberg-Bleyer et.al, Supplementary Materials (4 figures)

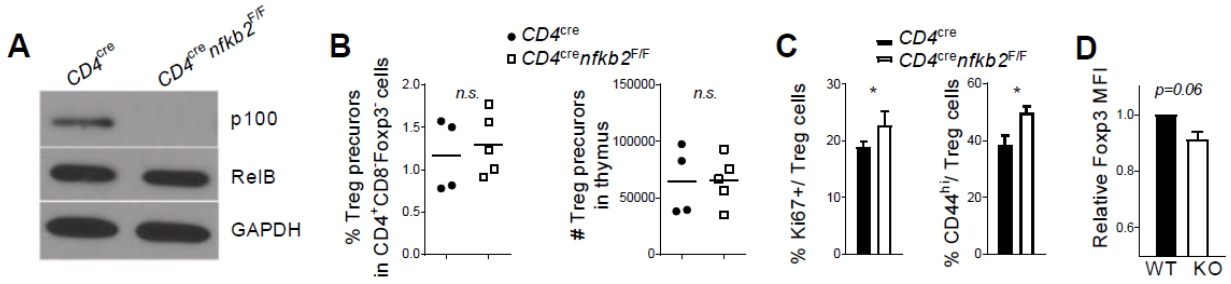

Figure S1. T-cell specific ablation of *nfkb2* drives peripheral Treg cell expansion

(A) Total splenic CD4$^+$ cells were sorted from *CD4*^{cre} and *CD4*^{cre}*nfkb2*$^{F/F}$ mice and lysed for Western Blot analysis. (B,C) Thymus and spleen of 6-8 weeks-old *CD4*^{cre} and *CD4*^{cre}*nfkb2*$^{F/F}$ mice were stained for FACS. (B) % (among CD4$^+$CD8$^-$Foxp3$^-$) and absolute number of CD25$^+$GITR$^+$ Treg precursors in the thymus. (C, D) % of Ki67$^+$ and CD44^{high} cells (C) and relative MFI of Foxp3 (D) in gated TCR-β^+CD4$^+$Foxp3$^+$ cells in the spleen. Data is from 2 to 3 independent experiments. In B, each dot represents a mouse. *p<0.05, n.s. : non-significant.

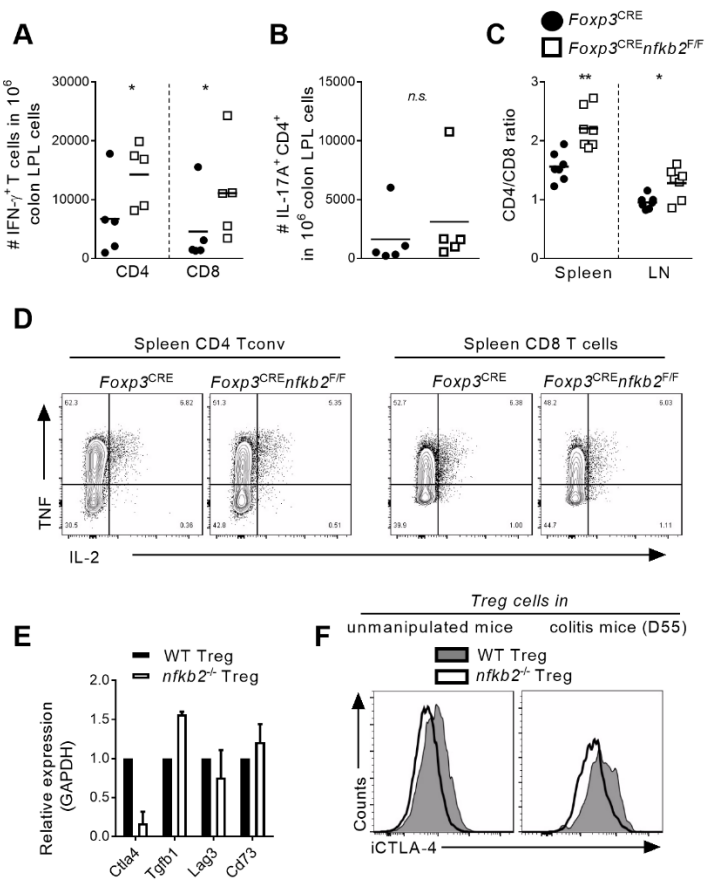

Figure S2. Uncontrolled inflammation in aging *Foxp3*^{cre}*nfkb2*$^{F/F}$ mice.

Tissues of 12-month old mice were stained for FACS. (A, B) Numbers of IFN-γ+ and IL-17A+ cell per 10^6 colon LPL cells (C) CD4/CD8 ratio in gated in TCR-β^+ live cells. Each dot represents a mouse from 3 pooled experiments. (D) Representative expression of TNF-α and IL-2 in gated spleen in TCR-β^+CD4$^+$Foxp3$^-$ (CD4) and TCR-β^+CD8$^+$ (CD8). Numbers indicate the % in each quadrant. No statistical difference was observed. Data is from 1 out of 2 experiments. (E) Splenic Treg were sorted from *Foxp3*^{cre} and *Foxp3*^{cre}*nfkb2*$^{F/F}$ mice, and gene expression was analyzed by q-RT-PCR. Expression of the given genes relative to the GAPDH control is shown. Mean +/-SEM of 2 experiments is shown. (F) Intracellular expression of CTLA-4 in gated CD45.2$^+$CD4$^+$Foxp3$^+$ of unmanipulated 12-month-old *Foxp3*^{cre} and *Foxp3*^{cre}*nfkb2*$^{F/F}$ mice (left) , and of recipient mice in the in vivo colitis assay (right). Data is representative of 2 experiments. *p<0.05,** p<0.005.

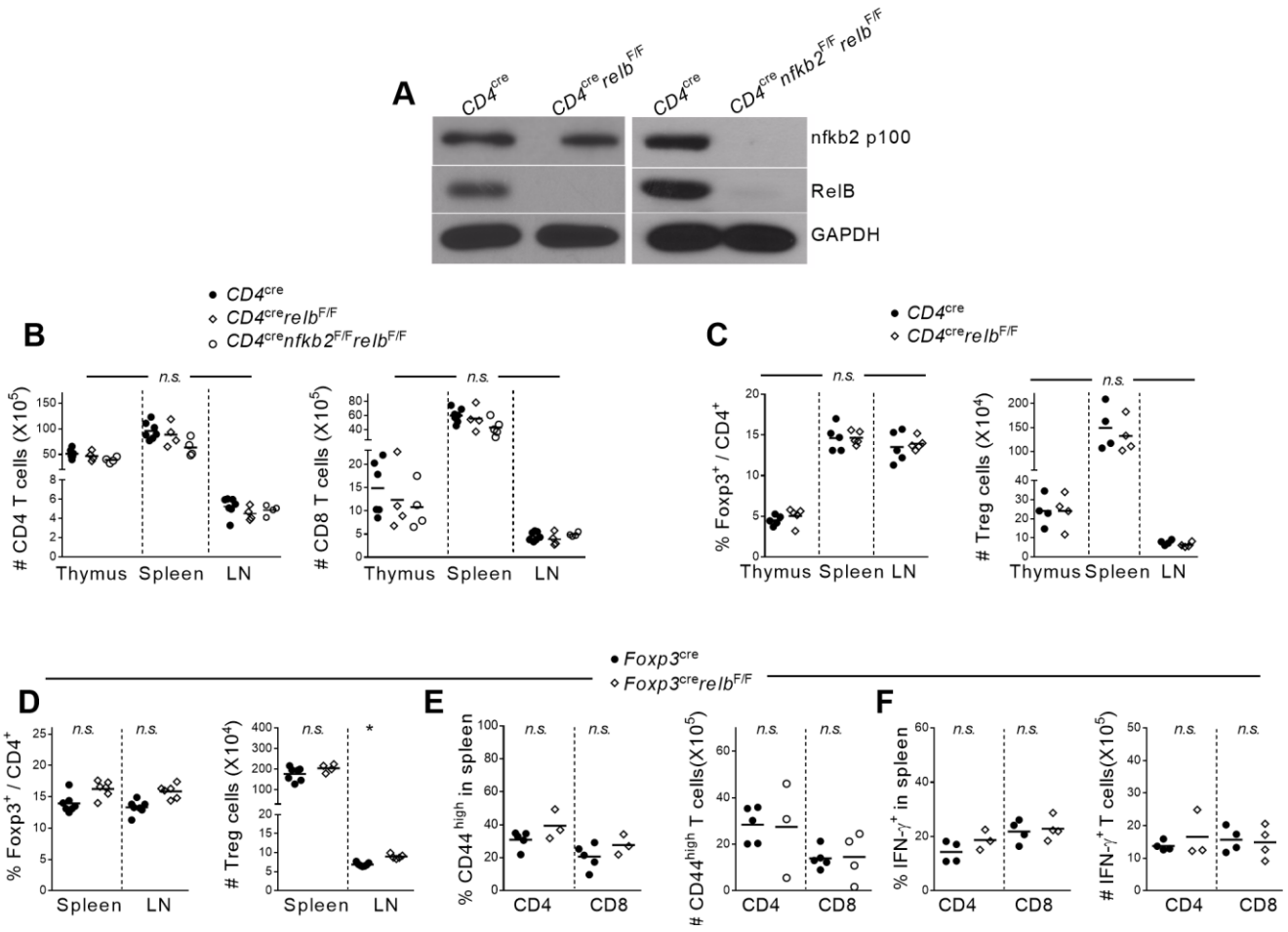

Figure S3. Overactivation of RelB in the absence of NF-κB2 drives uncontrolled Treg expansion and inflammation.

(A) Spleen CD4$^+$ cells were sorted from the indicated mice and lysed for Western Blot analysis. (B-C) Thymus, spleen and peripheral lymph nodes of 6-8 weeks-old *CD4*^{cre}, *CD4*^{cre}*relb*$^{F/F}$ and *CD4*^{cre}*nfkb2*$^{F/F}$*relb*$^{F/F}$ mice were stained for FACS. (B) Absolute numbers of live TCR-β$^+$CD4$^+$ and CD8$^+$ in the indicated tissues. (C) % in TCR-β$^+$CD4$^+$ and absolute numbers of Treg cells. (D-F) Tissues of 10-12-month-old *Foxp3*^{cre} and *Foxp3*^{cre}*relb*$^{F/F}$ mice were analyzed by FACS upon PMA-ionomycin restimulation. (D) % (in TCR-□$^+$CD4$^+$) and absolute numbers of Treg cells. (E-F) % (in CD4 and CD8 cells) and absolute numbers of CD44^{high} and IFN-γ$^+$ T cells, respectively. *p<0.05, n.s. : non-significant.

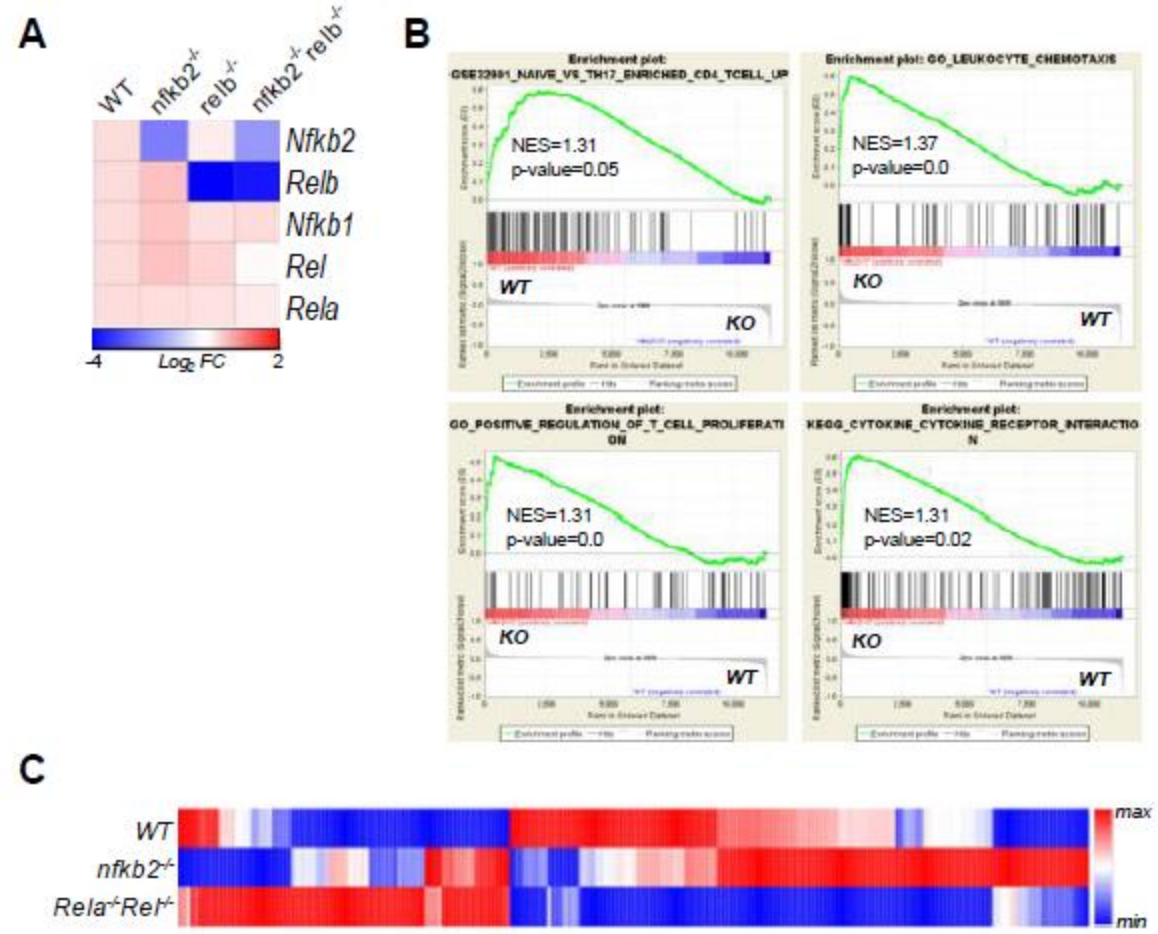

Figure S4. NF-κB2 represses aberrant expression of inflammatory and homing genes in Treg cells.

Treg cells were sorted from *Foxp3*^{cre}, *Foxp3*^{cre}*nfkb2*$^{F/F}$, *Foxp3*^{cre}*relb*$^{F/F}$ mice and *Foxp3*^{cre}*nfkb2*$^{F/F}$*relb*$^{F/F}$ mice, activated overnight and processed for RNA-seq. (A) Relative expression of NF-κB subunits. (B) Selected Gene Set Enrichment Analysis plots using genes with changed expression in *nfkb2*$^{-/-}$ Treg cells. The Gene Ontology, KEGG and Immunologic signatures Databases were screened. (C) Heatmap comparing the expression (fold changes) of genes with impaired expression in *nfkb2*$^{-/-}$ Treg cells, between WT, *nfkb2*$^{-/-}$ and *Rela*$^{-/-}$*Rel*$^{-/-}$ (*16*) RNAseq datasets.